

ARPES on $\text{Na}_{0.6}\text{CoO}_2$: Fermi surface, extended π band dispersion, and unusual band splitting

H.-B. Yang,¹ S.-C. Wang,¹ A.K.P. Sekharan,¹ H. Matsui,² S. Souma,² T. Sato,² T. Takahashi,² T. Takeuchi,³ J.C. Campuzano,⁴ R. Jin,⁵ B.C. Sales,⁵ D. Mandrus,⁵ Z. Wang,¹ H. Ding¹

(1) Department of Physics, Boston College, Chestnut Hill, MA 02467

(2) Department of Physics, Tohoku University, 980-8578 Sendai, Japan

(3) Research center for advanced waste and emission management, Nagoya University, Japan

(4) Department of Physics, University of Illinois at Chicago, Chicago, IL 60607

(5) Condensed Matter Science Division, Oak Ridge National Laboratory, Oak Ridge, TN 37831

The electronic structure of single crystals $\text{Na}_{0.6}\text{CoO}_2$, which are closely related to the superconducting $\text{Na}_{0.3}\text{CoO}_2 \cdot y\text{H}_2\text{O}$ ($T_c = 5\text{ K}$), is studied by angle-resolved photoelectron spectroscopy. While the measured Fermi surface is found to be consistent with the prediction of a local density band theory, the energy dispersion is highly renormalized, with an anisotropy along the two principle axes ($-\text{K}$, $-\text{M}$). Our ARPES result also indicates that an extended π band is formed slightly above E_F along $-\text{K}$. In addition, an unusual band splitting is observed in the vicinity of the Fermi surface along the $-\text{M}$ direction, which differs from the predicted bilayer splitting.

The recent discovery of superconductivity in $\text{Na}_x\text{CoO}_2 \cdot y\text{H}_2\text{O}$ ($T_c = 5\text{ K}$) [1] has generated great interests in the condensed matter physics community due to its potential connection to the high- T_c superconductivity. Over the past 17 years, the study of high- T_c superconductivity has focused on copper oxide compounds (cuprates). The unexpected finding of superconductivity in cobalt oxide (cobaltates) has raised the hope that it may help solve the high- T_c problem. Similar to the cuprates, Na_xCoO_2 has a layered structure. However, unlike the cuprates that have a square lattice in the plane, the cobaltate has a hexagonal lattice. For the electronic structure, both compounds have partially filled 3d orbitals, which form the low-energy excitations. In cuprates, Cu^{2+} has $3d^9$ configuration, and forms the highest e_g ($d_{x^2-y^2}$) band near E_F , with a strong hybridization to O 2p orbital. In cobaltates, the electronic configuration of Co^{4+} is $3d^5$, which occupies three lower t_{2g} bands, with the topmost band being $A_{1g} = (d_{xy} + d_{yz} + d_{zx})/\sqrt{3}$. The hybridization to the O 2p is greatly reduced due to the weaker overlap of the triangular bonding and the fact that the relevant orbitals in cobaltates are t_{2g} rather than e_g as in the cuprates.

In addition to these similarities in crystal structure and band orbitals, another important connection between the two materials is that both of them have strong electron correlations. It is widely believed that the physics of the high- T_c cuprates is that of a doped Mott insulator. It is believed that the cobaltate is also an electron-doped Mott insulator. The spin configuration in the frustrated half-filled triangular lattice may favor a RVB state [2], and superconductivity in the vicinity of such the RVB state may prefer a d-wave order parameter [3], similar to the cuprates. Moreover, the superconducting phase diagram of $\text{Na}_x\text{CoO}_2 \cdot 1.3\text{H}_2\text{O}$ is found to have a dome shape [4], which is also similar to the cuprates.

There also exist similarities between Na_xCoO_2 and another layered oxide superconductor Sr_2RuO_4 (ruthen-

ate), which is believed to be a p-wave superconductor. The two materials have similar behaviors in transport and magnetic susceptibility [6, 7]. In addition, both materials possess ferromagnetic fluctuations at low temperatures [8, 9], which are believed to be responsible for the p-wave pairing in the ruthenate. Thus a p-wave triplet superconducting state has been suggested for the cobaltate [5]. In addition, we note that both materials have the same electron filling level ($\frac{4}{3}$) for the maximum superconductivity. This is further away from half-filling than cuprates, in which the filling number of 1–0.16 is usually regarded as the optimal doping level.

Band structure and Fermi surface (FS) topology are known to be important for understanding unconventional superconductivity. Different electronic structures may induce different fluctuations, which can lead to different pairing symmetry. In this Letter, we report an angle-resolved photoelectron spectroscopy (ARPES) study on $\text{Na}_{0.6}\text{CoO}_2$ single crystals. Although $\text{Na}_{0.6}\text{CoO}_2$ is not a superconductor, a reduction of Na concentration and proper hydration can turn this material into a superconductor [1]. It is worth mentioning that $\text{Na}_{0.5}\text{CoO}_2$ has a large thermoelectric power ($S = 100\text{ mV/K}$ at 300 K), which is one order of magnitude larger than a typical S of metals and high- T_c cuprates [6]. In our ARPES study, we observe clear band dispersion and FS crossings in $\text{Na}_{0.6}\text{CoO}_2$. While the observed FS location is in a good agreement with the one predicted by LDA band theory [11], the observed bandwidth for the near- E_F band is renormalized and anisotropic along the two principle axes ($-\text{M}$, $-\text{K}$). The low-energy dispersion along $-\text{M}$ can be described by a simple tight binding t with a hopping integral $t = 44\text{ meV}$. The dispersion along $-\text{K}$ is more complicated, with an extended π band slightly above E_F and a break in dispersion around 70 meV. A tight binding t yields $t = 12 - 26\text{ meV}$, indicating a mass renormalization of a factor of 5–10. In addition, we observe an unusual band splitting along $-\text{M}$, which is however absent along $-\text{K}$.

High-quality $\text{Na}_{x}\text{CoO}_2$ single crystals are grown using the coating-zone method. The Na composition x 0.6, determined by inductively coupled plasma atomic emission spectroscopy. ARPES experiments are performed at the Synchrotron Radiation Center, Wisconsin. High-resolution undulator beam lines and Scienta analyzers with a capability of multi-angle detection have been used. Most spectra are measured using 22 eV photons. The energy resolution is 10 – 20 meV, and the momentum resolution 0.02 \AA^{-1} . Samples are cleaved and measured in situ in a vacuum better than 8×10^{-11} Torr at low temperatures (20 – 40 K) with a flat (001) surface. The sample is stable and shows no sign of degradation during a typical measurement period of 12 hours. The sample is oriented according to its Laue diffraction pattern, which shows a clear hexagonal lattice. LEED images obtained on fresh surface of cleaved samples also display a good hexagonal symmetry [10].

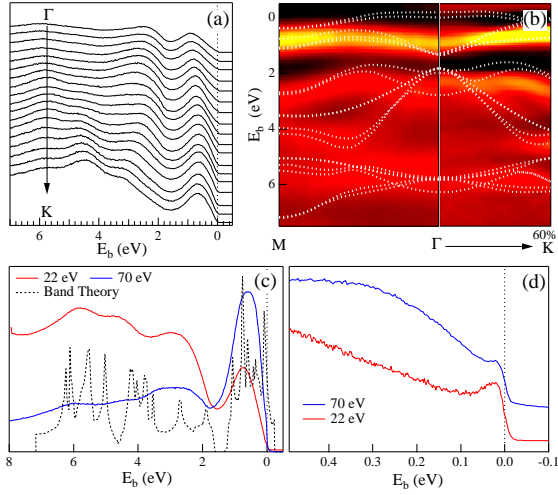


FIG. 1: Valence band of $\text{Na}_{0.6}\text{CoO}_2$. (a) EDCs along $-\text{K}$ ($h = 22 \text{ eV}$). (b) Intensity plots of the second derivatives of spectra along $-\text{M}$ and $-\text{K}$. (c) Integrated spectra over a large k -space for 22 eV (red) and 70 eV (blue) photons. The black dashed line is the total DOS from band theory [11]. (d) Near- E_F EDCs at k_F along $-\text{K}$ using 22 eV (red) and 70 eV (blue) photons.

In ARPES, a sign of a good surface is a clear valence band dispersion, which is observed in this material, as shown in Fig. 1. We measure the valence band at a number of photon energies, ranging from 16 – 110 eV. We find that, at low photon energies, the band dispersion is clearly visible, as shown in Fig. 1a where a set of energy distribution curves (EDCs) along $-\text{K}$ are measured with 22-eV photons. In Fig. 1b, we plot the intensity of the second derivatives of the measured EDCs to display band dispersion. It can be seen in Fig. 1b that the extracted band dispersion has many similarities with the calculated band structure [11]. However, the dispersion of the valence bands becomes less observable at relatively high photon energies ($h\nu > 70 \text{ eV}$). In Fig. 1c, we integrate spectra over a large k -space to mimic the density of

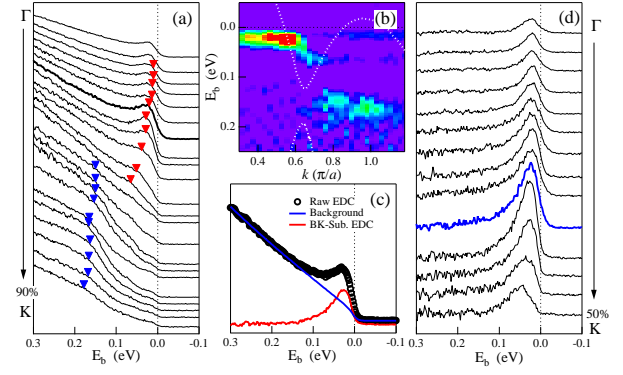


FIG. 2: Near- E_F spectra at 40 K along $-\text{K}$ ($h = 22 \text{ eV}$). (a) EDCs along $-\text{K}$. (b) Intensity plot of the second derivatives of the spectra shown in Fig. 2a. The white dashed lines are from the band calculation [11]. (c) An example of background subtraction. (d) EDCs after background subtraction. The blue curve is at $k_F = (0, 0.5)$.

states (DOS) for two different photon energies (22 and 70 eV). Four peaks can be identified at binding energies of 5.9, 4.6, 2.8, 0.7 eV respectively, matching well with the band calculation shown in Fig. 1c [11]. The band calculation shows that O 2p bands (2 to 7 eV) and Co 3d bands (below 2 eV) are well separated due to a weak Co d–O p hybridization. This is clearly reflected in Fig. 1c. In addition, a large enhancement of intensity for the 0.7-eV peak with 70-eV photons supports the Co 3d characters for this peak, since 70 eV is just slightly above the Co 3p–3d resonant excitation ($\sim 63 \text{ eV}$).

By examining the spectra in the vicinity of E_F , as shown in Fig. 1d, one can observe a weak but discernible peak sitting on a large “background” which is mainly a tail of the 0.7-eV peak, similar to an earlier ARPES measurement in a similar material [12]. According to the band calculation, this peak is the Co A_{1g} band which is at the top of Co t_{2g} manifold and forms a Fermi surface, and the large background is mostly t_{2g} bands. We find, as shown in Fig. 1d, that the Co 3p–3d resonant excitation does not help the enhancement of the A_{1g} peak since the resonance also enhances the background which has the same Co 3d character. Experimentally, we find that 22-eV photons yield the best result in identifying this near- E_F band.

Figure 2 shows dispersing spectra along a principle axis $-\text{K}$, or $(0,0) - (0, \frac{4}{3})$, in the hexagonal reciprocal lattice. The unit of k , used throughout this article, is π/a , where a (2.84 \AA) is the nearest Co–Co distance. As seen in Fig. 2a, a “shoulder-like” peak centered around 65 meV starts to emerge at $k = (0, 0.66)$. With decreasing k_y , this peak disperses toward E_F , and seems to cross E_F at $(0, 0.5)$. Note that another broad peak around 160 – 200 meV emerges at $k_y > 0.8$, which has no smooth connection to the A_{1g} band. A careful examination of the spectra indicates that there is a “break” in dispersion, as shown in Fig. 2b. Comparing to the calculated band dispersion along $-\text{K}$, this “break” occurs at almost the same k -location where the A_{1g} band intersects with

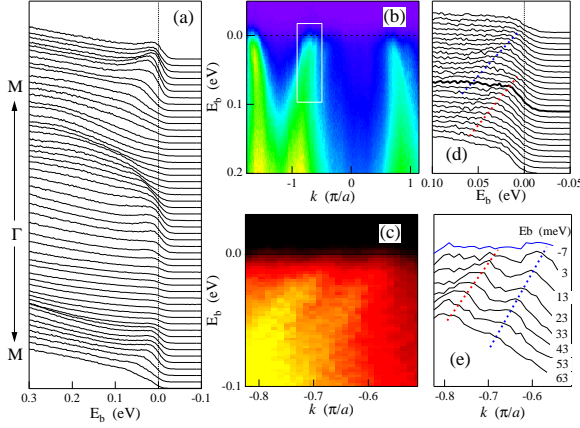


FIG. 3: Near- E_F spectra at 40 K along $-M$. (a) EDCs and (b) E-k intensity plot for a long cut along $M - M$. Plots of (c) E-k intensity, (d) EDCs, (e) MDCs magnified from the white box in Fig. 3b. Dashed lines are the guides for peak positions.

another t_{2g} band. Therefore, this "break" might be a consequence of the mixing of the two bands. The second t_{2g} band is predicted to cross the Fermi energy and form a small Fermi surface pocket near the K point. However, no evidence of this FS crossing is observed in our experiment, which could easily result from a slight shift in the chemical potential. Another possible explanation for the "break" in dispersion is that the electron band interacts with collective modes, such as phonon modes. Three phonon modes, with the energy of $\sim 55 - 75$ meV, have been observed by a Raman experiment [13].

To see the low-energy excitation more clearly, we subtract the large "background" from an EDC. One example of the subtraction is demonstrated in Fig. 2c where an almost straight line is used for the background. The background-subtracted EDCs along $-K$ are plotted in Fig. 2d. One can clearly see that an asymmetrical peak disperses toward E_F while its lineshape sharpens up. At $k = (0, 0.5)$, the peak experiences a substantial reduction in its intensity, indicating that the peak is crossing E_F and the sharp Fermi function removes most of spectral weight above the E_F . After the crossing, a small peak near E_F persists for an extended range of k , from $(0, 0.5)$ to $(0, 0)$. This indicates that there is an extended "at band" just above the E_F . The small peak is the left-over intensity from the Fermi function cutoff. We note that there is an extended "at band" in both cuprates (i.e. $Bi_2Sr_2CaCu_2O_8$) and ruthenate Sr_2RuO_4 . While the influence of the "at band" to superconductivity is still under debate, the enhanced DOS near E_F would certainly enhance spin and charge fluctuations, which are found to be strong in all of the three materials.

ARPES spectra along another principle axis $-M$, or $(0, 0) - (\frac{\pi}{3}, 0)$, are plotted in Fig. 3. Symmetric dispersion can be observed along a long cut in k over different Brillouin zones (BZs). We observe some differences for spectra between $-M$ and $-K$. One major difference is that there is a band splitting along $-M$. This splitting

can be easily seen if we zoom in at the band crossing, as shown in Fig. 3 (c) to (e) where we plot an intensity plot, EDCs, and momentum distribution curves (MDCs) in the vicinity of the band splitting. From these three displays, we observe two nearly parallel bands in the vicinity of k_F with an energy separation of ~ 60 meV and a momentum separation of $\sim 0.1 \pi/a$.

We summarize our ARPES results in Figure 4. In Fig. 4a, we plot the FS crossings (FSCs) in the hexagonal BZ. For comparison, the calculated FS of $Na_{0.5}CoO_2$ is also plotted in Fig. 4a [11]. We have measured many samples on several photon energies, with consistent results. All the FSCs shown in Fig. 4a are extracted directly from measurements, and no symmetry operations have been applied here. Note that the FSCs with same symbols over different BZs are obtained from a same sample during a short time interval. This eliminates potential problems from sample misalignment and surface contamination, and helps to accurately determine the size of the FS. As seen from Fig. 4a, the size of measured FS in $Na_{0.6}CoO_2$ is slightly larger than the calculated one in $Na_{0.5}CoO_2$. We also notice that in a recent ARPES study for a more Na-doped sample ($Na_{0.7}CoO_2$), the observed hole-like FS appears larger than the one observed here [19]. The conclusion of having a smaller occupied area for more doped electrons from Na apparently violates the Luttinger theorem. It is possible that some electron carriers become localized at higher Na doping levels, resulting a reduction in the number of itinerant electrons which contribute the area of the FS. This might also explain the unusual ferromagnetic transition observed in highly Na-doped samples [20, 21].

We extract band dispersion from peak positions in MDCs. The extracted band positions along $-M$ and $-K$ are plotted in Fig. 4b and c. Reliable values of the dispersion can be extracted from E_F to ~ 70 meV since beyond this energy the spectral linewidth becomes so broad that its position is ill-defined. As seen in Fig. 4b, the measured band dispersion along $-M$ is nearly linear for the 70 -meV range, with a Fermi velocity $v_F \sim 0.41$ eV/Å. We use a simple tight binding band for the triangular lattice to fit the measured band dispersion for the outer band,

$$E_k = -2t(\cos k_x + 2 \cos \frac{k_x}{2} \cos \frac{3k_y}{2}) \quad (1)$$

where t is the nearest neighbor hopping integrals, and the chemical potential. The fitting result yields $t \sim 44$ meV (with a negative sign) along $-M$. The measured dispersion along $-K$ is more complicated, as shown in Fig. 4c. In addition to the "at dispersion" around 70 meV due to the "break", the dispersion changes its slope at ~ 20 meV. This slope change may be a consequence of the "at band" observed in Fig. 2. While a tight binding fit for the range between E_F and 20 meV yields $t \sim 12$ meV and $v_F \sim 0.12$ eV/Å, another fit for the range between 20 to 70 meV produces $t \sim 26$ meV and $v_F \sim 0.24$ eV/Å. Both values of t are smaller than the one along $-M$. The different values of t along the two princi-

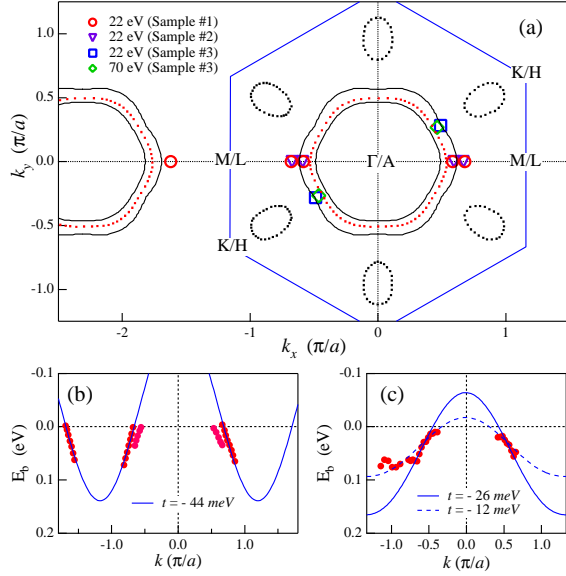


FIG. 4: (a) Measured FS crossings (symbols) comparing to the calculated FS in $k_z = 0$ (black solid lines) and $k_z = 0.5$ (red dashed lines) planes. The blue hexagon is the 2D Brillouin zone. (b) Extracted band positions along $-M$ (red dots) and a tight binding t with $t = -44$ meV (solid line). (c) Extracted band positions along $-K$ (red dots) and two tight binding t s with $t = -12$ meV (solid line) and $t = -26$ meV (dashed line).

ple axes are unexpected from a simple tight binding t or LDA band theory. This indicates that either t is k -dependent, or there may be other factors that modify the band dispersion, such as low-lying modes or energy gaps.

The small value of t , especially along $-K$ ($t = -12$ to -26 meV), is puzzling. It is estimated that the superexchange interaction J is 12 and 24 meV in Na_xCoO_2 [3]. Apparently, the small t observed here is the effective t_{eff} , which is renormalized from the original band t , estimated to be 130 meV (the total band width is $12t = 1.6$ eV) [11, 14]. The reduction of t indicates a strong mass renormalization of a factor of 5–10, which is likely due to the strong correlation in this material. A similar mass renormalization (~ 7) is also suggested by a large electronic specific heat coefficient (~ 48 mJ/molK²) observed in

this material [15, 16]. We note that both the flat section of the FS and the extended flat band observed along $-K$ would make it the dominant direction in contribution to the DOS. Therefore, t along $-K$ is more relevant to the specific heat result.

Perhaps more surprising finding from this study is a relatively large band splitting along M . While band theory predicts a bilayer splitting resulting from the two CoO_2 planes per unit cell [11], we cast some doubts to this assignment due to the following reasons. (1) In the case of the bilayer splitting, the c -axis hopping integral t_c would be 30 meV, similar to the in-plane t . This is inconsistent with the large transport anisotropy ($\rho_{ab} = \rho_c \sim 200$ at 4 K) [6]. (2) Perhaps more importantly, the two CoO_2 layers in a unit cell have identical geometry for Co atoms, and this would not generate a bilayer splitting for the Co A_{1g} band near E_F which has very small overlap with oxygen orbitals. In support of this, we note that the band calculation shows no discernable gap at the zone boundary of the doubled unit cell [11]. This suggests that the band can be unfolded to yield a c -axis dispersion rather than a splitting. (3) No band splitting is observed along K , which is not consistent with a simple bilayer splitting, although different k_z may modify the size of splitting. It is known that other phenomena, such as itinerant ferromagnetism, can also cause band and FS splitting. Several experiments have detected ferromagnetic fluctuations at low temperatures in this material [9, 18]. Although speculative, it is possible that this fluctuation may order on the surface, causing a ferromagnetic band splitting. More studies are necessary in order to resolve this issue.

We thank M. Fisher, C. Gundlach, and H. Hochst for technical support in synchrotron experiments, P.D. Johnson, P.A. Lee, N.P. Ong, D.J. Singh, and J.D. Zhang for useful discussions and suggestions. This work is supported by NSF DMR-0072205, DOE DE-FG02-99ER45747, Petroleum Research Fund, Sloan Foundation. The Synchrotron Radiation Center is supported by NSF DMR-0084402. Oak Ridge National Laboratory is managed by UT-Battelle, LLC, for the U.S. Department of Energy under contract DE-AC05-00OR22725.

[1] K. Takasa et al., Nature 422, 53 (2003).
[2] G. Baskaran, cond-mat/0303649, 2003.
[3] Q. H. Wang, D. H. Lee, and P. A. Lee, cond-mat/0304377, 2003.
[4] R. E. Schaak et al., Nature 424, 527 (2003).
[5] D. J. Singh, Phys. Rev. B 68, 020503 (2003).
[6] I. Terasaki, Y. Sasago, and K. Uchinokura, Phys. Rev. B 56, R12685 (1997).
[7] Y. Maeno et al., Nature 372, 532 (1994).
[8] T. Imai et al., Phys. Rev. Lett. 81, 3006 (1998).
[9] K. Ishida et al., cond-mat/0308506, 2003.
[10] J.D. Zhang, private communication.
[11] D. J. Singh, Phys. Rev. B 61, 13397 (2000).
[12] T. Valla et al., Nature 417, 627 (2002).

[13] M. N. Iliev et al., cond-mat/0308065, 2003.
[14] J. Kunes, K.-W. Lee, and W. E. Pickett, cond-mat/0308388, 2003.
[15] Y. Ando et al., Phys. Rev. B 60, 10580 (1999).
[16] F. C. Chou et al., cond-mat/0306659, 2003.
[17] H. Ikeda, Y. Nisikawa, and K. Yamada, cond-mat/0308472, 2003.
[18] R. Jin et al., cond-mat/0306066, 2003, Phys. Rev. Lett., in press.
[19] M. Z. Hasan et al., cond-mat/0308438, 2003.
[20] T. Motohashi et al., Phys. Rev. B 67, 064406 (2003).
[21] J.L. Gavilano et al., cond-mat/0308383, 2003.